Journal of Building Engineering 80 (2023) 108002

Contents lists available at ScienceDirect

Journal of Building Engineering

journal homepage: www.elsevier.com/locate/jobe

Analysis of parameters influencing pathogen concentration in a room with displacement ventilation using computational fluid dynamics and Taguchi methods

Bahadir Erman Yuce [a,b,*], Amar Aganovic [c], Peter Vilhelm Nielsen [d], Pawel Wargocki [b]

[a] Faculty of Engineering and Architecture, Mechanical Engineering Department, Bitlis Eren University, Rahva Campus, Bitlis, 13100, Türkiye
[b] International Centre for Indoor Environment and Energy, Department of Environmental and Resource Engineering, Technical University of Denmark, Kongens Lyngby, 2800, Denmark
[c] Department of Automation and Process Engineering, The Arctic University of Norway, Tromsø, Norway
[d] Department of the Built Environment, Aalborg University, Aalborg, 9220, Denmark

ARTICLE INFO

Keywords:
Computational fluid dynamics
Taguchi
Ventilation
Covid-19
Optimization
Wells-Riley

ABSTRACT

Analyzing multiple physical factors simultaneously to determine optimal ventilation solutions can be challenging. Furthermore, this type of analysis needs a large case number to be investigated, making the problem's solution unfeasible. This study tackled these challenges by integrating Computational Fluid Dynamics (CFD) with the Taguchi method to overcome these issues. Our previous research extensively examined the application of the Taguchi method in ventilation studies. Now, we analyzed the influence of different factors on pathogen concentration in a room equipped with displacement ventilation. Initially, the study examined the effects of room dimensions and the location, position, velocity, and temperature of the inlet and outlet of the ventilation system. The Taguchi method was employed to manage the complexity of the analysis, resulting in a reduced set of 27 cases from a total of 19683 possible combinations. The findings revealed that the inlet velocity was the most influential parameter in minimizing pathogen concentration; however, room volume has a limited effect. Subsequently, the optimal solution obtained through the Taguchi method was modeled using CFD and validated. Then, these results were compared against the results of the Wells-Riley model, which utilized room volume and inlet velocity as input variables. In the second step, additional parameters were investigated while keeping the room volume constant. This analysis reaffirmed the significant impact of inlet velocity on pathogen concentration, as observed in the initial study. Additionally, it was found that inlet temperature had a greater influence on pathogen concentration in rooms with smaller dimensions.

1. Introduction

The World Health Organization (WHO) declared a global epidemic of Covid-19, On March 11, 2020. Human coronaviruses were known before this pandemic but not considered fatal before 2003 and were even known as mild illnesses like the common cold [1,2].

* Corresponding author. Faculty of Engineering and Architecture, Mechanical Engineering Department, Bitlis Eren University, Rahva Campus, Bitlis, 13100, Türkiye.
E-mail address: beyuce@beu.edu.tr (B.E. Yuce).

https://doi.org/10.1016/j.jobe.2023.108002
Received 13 July 2023; Received in revised form 2 October 2023; Accepted 21 October 2023
Available online 30 October 2023

After this date, severe acute respiratory syndrome (SARS) and the Middle East respiratory syndrome (MERS) outbreaks showed that human coronaviruses can be dangerous and devastating [2].

Various measures have been taken to stop the epidemic in many countries after the declaration of the SARS-COV-2 pandemic. Multiple restrictions were imposed on restaurants, schools, cinemas, congress centers, and many other spaces closed, and social distancing, masks, and vaccinations were mandatory for many activities. Despite all these measures, many people around the world have died. Social wellness and economic development had been affected significantly [3,4]. The inevitable consequences of the pandemic and the measures taken have encouraged researchers to research more in this area to understand the physics of the transmission and prevent this and future epidemics.

According to the World Health Organization, the spread of SARS-CoV-2 occurs when an infected person is in close contact with other people. Transmissibility of the virus depends on the amount of live virus expelled and shed by a person, the type of contact, the environment, and what IPC (Infection, prevention, and control) measures are applied. The transmission of the virus can occur through the expulsion of tiny liquid particles from an infected individual's mouth or nose during various activities such as coughing, sneezing, taking deep breaths, singing, or engaging in conversation. These liquid particles exhibit a range of sizes, encompassing larger respiratory droplets and smaller airborne particles known as 'aerosols' [5]. The droplet size-based classification system for respiratory disease routing was first reported by Wells [6] in the 1930s on tuberculosis transmission [1]. Tang et al. defined aerosols as poly-dispersed droplets and particles of many sizes [7]. This study focused on aerosols with the definition of infectious respiratory aerosol droplets with aerodynamic diameter <5 μm.

Ventilation is a critical engineering solution to minimize the infection risk in the indoor environment. Many researchers have suggested that increasing the amount of fresh air given to the buildings from the ventilation systems decreases the infection risk in buildings [8–11]. Since the early 2000s, there has been an increase in studies examining the effect of indoor ventilation on airborne transmission. With the 2002–2003 SARS virus epidemic, the focus on this area increased, and with the pandemic that occurred in 2019, studies in this area have diversified significantly. In addition to different interior spaces such as classrooms [12,13], offices [14,15], restaurants [9], hospital rooms [8,16], ophthalmology clinics [17], dental clinics [18], and aircraft [19–21], bus [22,23] and train cabins [24,25], different topics such as exposure type and severity [26], and social distance [27,28] have been studied by many researchers. Most of the studies are parametric, and it is aimed to find a scenario that will minimize the risk of contamination according to the title examined. There are also studies in which the most suitable parameters are tried to be obtained by changing the inlet velocity [8,12], relative humidity [29,30], ventilation type [14,28,31,32], and inlet or outlet positions [15]. The results obtained from these studies are very important so that the existing systems can be used to minimize the infection risk. On the other hand, these studies generally were applied to certain interior spaces and the results were limited to the model used. In addition, it is often difficult to compare the different parameters studied, again for this reason.

Displacement ventilation (DV) has been a popular choice for ventilation in industrial premises for many years, and since the mid-80s, it has also gained popularity in non-industrial settings. One of the advantages of using DV is that it provides the opportunity to enhance both temperature control and ventilation efficiency. As a result, the air quality in the occupied zone is typically better when using DV compared to traditional mixing ventilation (MV) systems [33]. How contamination is distributed throughout a displacement-ventilated room is closely tied to the placement of sources of contamination and whether or not any sources of heat are also sources of pollution. When warm sources of pollution are concentrated in a specific area, all of the contaminants can be carried directly into the upper zone of the room through convection flows and this is considered to be the ideal scenario for DV [34]. In an operating microenvironment where cold air is introduced and comes into contact with a heat source, the resulting temperature difference and buoyancy force can cause contaminated air to rise upward and accumulate near the ceiling of the room. This warm and polluted air can then be effectively removed from the space through an outlet that is located close to the ceiling [35]. Studies in the literature focused on many factors that can affect the pathogen concentration in the room as the distance between the source and target [36], the positions of the manikins, and the effect of moving [37]. Moreover, several studies in the literature have suggested that DV systems are more effective than MV systems in reducing the risk of airborne infections [38,39].

Statistical methods can be used to determine ventilation parameters that will minimize infectious concentration. Although Taguchi's method is not common in ventilation studies, it is frequently used in other research areas [40–44]. It is possible to evaluate the effect of independent ventilation parameters on the concentration in detail with the Taguchi method. In our previous study, we extensively examined the application of this method by employing a well-known benchmark case [45]. Another advantage of this method is that it is possible to solve a limited number of cases without solving every combination of different values of the parameters [45]. There are few studies on this subject and methodology in numerical ventilation studies [46–51].

In this study, we adopted an exploratory and novel approach with a primary focus on applying the Taguchi method to minimize infectious disease transmission within indoor environments. To gain a comprehensive understanding of the effectiveness of various design parameters, we examined an extensive range of parameters using the Taguchi method. This approach enabled us to encompass a wide range of solutions, thereby providing more general insights within the examined scenarios and parameters. In other optimization studies, depending on the methodology, a large solution space has been usually examined. To reduce the optimization boundaries, studies performed previously that used similar methodologies in their analyses have been taken into account, and the parameter range could be reduced on these criteria. Because the method in this study is novel in the field of airborne transmission and ventilation, we could not use a similar approach. We believe that the present study will be considered as providing useful resource by future studies.

This study's core objective was to assess the impact of design parameters on airborne pathogen concentration using a combination of CFD and statistical methods. This approach allowed us to consider the chaotic air flow movements stemming from turbulent flow within indoor spaces. An extensive array of parameters was meticulously examined using the Taguchi method to gain a comprehensive understanding of the effectiveness of these parameters in reducing pathogen concentration, quantitatively represented by the CO2

mass fraction. These quantitative results could serve as a foundational resource for identifying crucial approaches to reducing the probability of airborne transmission within enclosed spaces. Potential strategies include room design modifications, temperature setting optimization, increased outdoor air supply rates, and other pertinent considerations.

Additionally, the best parameter conditions obtained from the Taguchi method were numerically analyzed, and it was verified that the average concentration value obtained in this case was the minimum value. In order to support the research findings about the impact of inlet velocity and room volume on pathogen concentration, the Taguchi method was additionally applied to the Wells-Riley method, an infection risk prediction model. It was observed that impact ratios of inlet velocity and room volume on pathogen concentration obtained from the Wells-Riley method were compatible with the results of the present study. In conclusion, this study aimed in providing the guidance for implementation of practical solutions and stimulating future work depending on the impact ratio of ventilation parameters on pathogen concentration.

2. Methodology

The evaluation of airborne transmission and ventilation characteristics, including inlet velocity, inlet temperature, manikin position, positions of inlet and outlet, and room dimensions, was conducted using CFD and Taguchi methods. The study focused on a DV setup and considered two separate cases. In the first case, the influence of room volume on pathogen concentration was found to be minimal, as elaborated in the Results section. However, specific parameters could not be examined due to the limitations of the statistical model employed. To address this, a smaller fixed-volume room was investigated, wherein low-impact parameters were eliminated while new parameters were introduced. This expansion of the study's scope facilitated the acquisition of further data.

For the 1st case, all parameters were examined with different levels, and these values are shown in Table 1. Room length and width are defined according to one-person office sizes of Bitlis Eren University, Faculty of Engineering and Architecture. Room height values of the offices were constant at 3 m. Other values were obtained from other buildings on the Campus. Inlet velocity values are defined for the different ACH values between 4 and 69. A broad range of temperature values was assigned to the inlet air, mirroring the approach taken with other parameters. The use of larger ranges allowed for a detailed investigation into the impact of each parameter. As the primary focus of this study was on the relationship between pathogen concentration and thermal turbulent flow, considerations regarding thermal comfort limits were not taken into account. It is anticipated that future studies will explore standards and thermal comfort limits based on the outcomes obtained in this research.

ANSYS Fluent 2021 R1 was used to solve governing equations. CFD settings and software were validated with the velocity and temperature measurements of the two-dimensional benchmark test case of Nielsen [52].

2.1. Numerical setup

The fluid flow was considered steady state and turbulent. The standard k-ε turbulence model was used as a turbulence model, and the scalable wall function was selected [53]. The scalable wall function was used to obtain accurate mesh around the complex manikin surface and its good performance from studies in the literature [54]. All walls were considered adiabatic, and no-slip boundary conditions were applied. CO_2 was selected as a tracer gas to simulate the contaminants in the exhaled airflow. The Species Transport Model was used to solve CO_2 distribution in the room [55]:

$$\frac{\partial}{dt}(\rho Y_i) + \nabla.(\rho \vec{v} Y_i) = -\nabla.\vec{J}_i + R_i + S_i \tag{1}$$

Where ρ is the fluid density, Y_i is the local mass fraction, $\vec{v}$ is the velocity vector, R_i is the net rate of production, $\vec{J}_i$ is the diffusion flux of CO_2 and S_i is the rate of the source.

Firstly, the pressure-velocity coupling scheme was selected as Simple, and First Order Upwind spatial discretization was selected for turbulent kinetic energy, momentum, energy, turbulent dissipation rate, and CO_2. The result of this solution setup was used as the initial value for the final solution setup in which the Couple scheme and Second Order Upwind spatial discretization were used. Convergence criteria were defined as 10^{-6} for all equations.

The Boussinesq model was applied to define buoyancy-driven flow in the room and the thermal plume of the manikin. Air properties were determined according to inlet temperature, and thermo-physical properties of air were obtained from Cengel [56].

Table 1
Parameters and their levels for 1st case.

Parameters	Levels		
	1	2	3
Inlet velocity (m/s)	1	3	5
Inlet temperature (°C)	18	22	26
Inlet height (m)	0	0.2	0.4
Inlet location (m)	M	R	L
Outlet Height (m)	0	0.2	0.4
Outlet location (m)	M	R	L
Room length (m)	3	4	5
Room height (m)	2.4	2.7	3
Room width (m)	2.5	3	3.5

Grid independence was obtained for each case accordioning to average CO_2 mass fraction values.

2.2. Boundary conditions

The numerical model is based on an office room with a sitting thermal manikin. For the 1st case, the thermal manikin was positioned in the center of the room and facing the air inlet. Three different inlet and outlet positions (middle-M, right-R, and left-L side of the front face) were investigated at three different distances from the floor and ceiling (0, 0.2, 0.4 m). Inlet velocity (1, 3, 5 m/s) and temperature (18, 22, 26 °C) were also investigated with three different values. These different room volume and inlet velocity values correspond to an extensive range of ACH to investigate. The surface of the manikin is maintained at a constant temperature of 35 °C All inlet and outlet positions are shown in Fig. 1. In the study, boundary conditions were simplified in both cases due to the lack of a specific aim for cross-infection, and only the mouth was modeled. However, we would like to remind researchers that this modeling approach is critical in cross-infection studies [57].

2.3. Contaminant source and tracer gas approach

Compared to other occasional respiratory activities such as sneezing or coughing, human exhaled breaths have the potential to contain the largest droplets and volume of air in total [58], and according to the findings of Ma et al., COVID-19 patients release SARS-CoV-2 directly into the air through the breathing [59].

Papineni and Rosenthal (1997) examined the droplets from human subjects performing four respiratory actions with optical particle counter tests, and they stated that the preponderance of particles is less than 1 μm. However, larger particles were also detected [60]. Bivolarova et al. measured the concentration of aerosol particles with different diameters (0.07, 0.7, and 3.5 μm) and a tracer gas (nitrous oxide - N2O) in a test room with mixing ventilation. According to their statement, particles within the fine size range (0.7 μm) are minimally affected by deposition mechanisms and are expected to exhibit similar behavior to the tracer gas. They also emphasized the significance of ventilation rate when comparing the behavior of ultrafine particles and tracer gas, but the ventilation rates they studied did not have a significant effect on the 3.5 μm and the 0.7 μm particles [61]. Li et al. (2011, 2013) used the CFD and showed that exposure of particles not larger than 2.5 μm and spatial distribution of tracer gas (CO_2) results were very close to each other in their study [62,63]. Yin et al. (2011) also experimentally compared the distribution profiles of the sulfur hexafluoride (SF6) tracer gas and 1 and 3 μm particles in a patient ward. In their findings, it was observed that the contaminant concentration profiles in the room appeared similar, except in the regions near the source of contamination and exhaust, where the airflow exhibited instability [64]. Another study showed that smaller particles (0.5–10 μm) may remain suspended more than larger particles and contribute to transmission over greater distances [65]; this dynamic behavior is also similar to those of gaseous agents, which make them more influenced by airflow patterns and ventilation rates [66]. In another study, it was demonstrated that non-equilibrium droplet evaporation was not observed for particles ranging from 0.5 to 20 μm [67].

As a result, the tracer gas method was used because of its very advantageous features to model airborne transmission, such as its lower computational cost, and its physical behavior similar to small diameter particles that are more sensitive to airflow. In addition, although the tracer gases and the droplets have physical differences such as evaporation and deposition, these differences can be neglected due to the transmission mechanism of small aerosols. This study used carbon dioxide (CO_2) as a tracer gas [16,68,69]. Manikin mouth was considered a contaminant source with 97 mm^2 to simulate the exhaled contaminants by infected manikin under different ventilation conditions. The flow rate of CO_2 was considered as 0.6 l/min and exhalation temperature is 35 °C.

2.4. Taguchi method

Taguchi method [70] has wide usage in many research fields mainly because of its performance in many studies [40–44]. The order

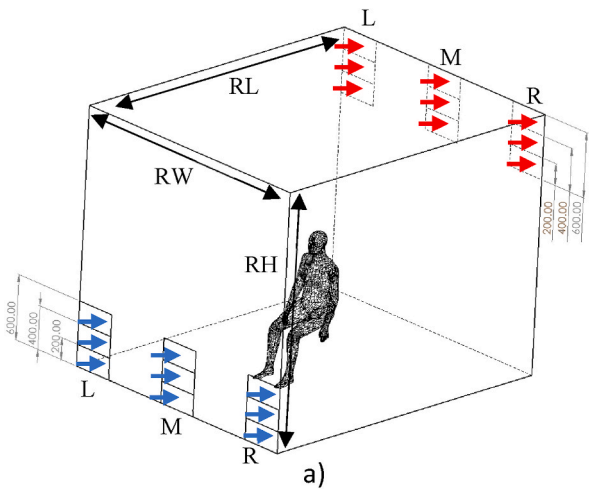

Fig. 1. Room model and inlet and outlet positions for the 1st case.

of importance for investigated parameters which are also independent of each other can be obtained Taguchi method [71]. In addition, the Taguchi method provides a set of parameters that will produce the best-case scenario.

In the present study, the Taguchi method calculation procedure encompassed four distinct steps, carried out in the following sequence: the establishment of an orthogonal array definition, computation of signal-to-noise (S/N) ratios for each factor under investigation, derivation of delta values based on the S/N ratios, and determination of the order assigned to each factor. Yuce et al. examined these steps in detail [45] for a numerical ventilation study.

The S/N ratio is characterized in three distinct forms in this context: the lower is the better, the nominal is the best, and the larger is the better [72]. The approach employed in this study is the "smaller is better" to minimize tracer gas concentration, and it is defined below:

The smaller the better [40]:

$$S/N = -10\,log\left(\frac{1}{n}\sum_{i=1}^{n} Y_i^2\right) \tag{2}$$

The value Yi denotes the outcome for the objective function corresponding to the ith case.

The ranking is determined by calculating the delta values, which are obtained by subtracting the minimum S/N value from the maximum S/N value for each parameter. The parameter with the highest delta value signifies the most influential one, and the rank is assigned accordingly.

To explore the entire parameter space with fewer experiments, the Taguchi method employs a unique design of orthogonal arrays, significantly reducing the required number of experiments to solve the problem [73]. In the current study, an orthogonal array was chosen based on the total degree of freedom (DOF) criterion. The DOF for each factor can be calculated as one less than the number of factor levels [74]' this value should be smaller than the DOF of the chosen orthogonal array. Consequently, DOF was calculated to be 26 in the present study. L27(3^9) Taguchi orthogonal array with 27 cases and nine parameters with three levels, is used and shown in Table 2.

2.5. Wells-Riley method

In this study, the Wells-Riley method was employed as a means to verify the results obtained from computational fluid dynamics (CFD). The Wells-Riley method is a quantitative prediction technique for assessing infection risk, which relies on the concept of quanta. Quanta refers to the number of infectious airborne particles necessary to infect an individual [75]. Specifically, it represents, in 63 % of susceptible individuals, it denotes the dose of airborne droplet nuclei necessary to induce infection [76].

To calculate the probability of infection risk associated with different ventilation rates and room volumes, a standard airborne Wells-Riley model was utilized. This model was calibrated to account for COVID-19 and incorporated relevant quanta emission rates

Table 2
Room model and inlet and outlet positions for the 1st case.

Case number	Inlet velocity (m/s)	Inlet temperature (°C)	Inlet height (m)	Inlet location	Outlet Height (m)	Outlet location	Room length (m)	Room height (m)	Room width (m)	CO_2 (mass fraction)
1	1	18	0	M	0	M	3	2.4	2.5	0.00166
2	1	18	0	M	20	R	4	2.7	3	0.00198
3	1	18	0	M	40	L	5	3	3.5	0.00178
4	1	22	20	R	0	M	3	2.7	3	0.00234
5	1	22	20	R	20	R	4	3	3.5	0.00210
6	1	22	20	R	40	L	5	2.4	2.5	0.00266
7	1	26	40	L	0	M	3	3	3.5	0.00203
8	1	26	40	L	20	R	4	2.4	2.5	0.00200
9	1	26	40	L	40	L	5	2.7	3	0.00180
10	3	18	20	L	0	R	5	2.4	3	0.00066
11	3	18	20	L	20	L	3	2.7	3.5	0.00064
12	3	18	20	L	40	M	4	3	2.5	0.00061
13	3	22	40	M	0	R	5	2.7	3.5	0.00075
14	3	22	40	M	20	L	3	3	2.5	0.00043
15	3	22	40	M	40	M	4	2.4	3	0.00052
16	3	26	0	R	0	R	5	3	2.5	0.00068
17	3	26	0	R	20	L	3	2.4	3	0.00078
18	3	26	0	R	40	M	4	2.7	3.5	0.00069
19	5	18	40	R	0	L	4	2.4	3.5	0.00037
20	5	18	40	R	20	M	5	2.7	2.5	0.00033
21	5	18	40	R	40	R	3	3	3	0.00044
22	5	22	0	L	0	L	4	2.7	2.5	0.00048
23	5	22	0	L	20	M	5	3	3	0.00038
24	5	22	0	L	40	R	3	2.4	3.5	0.00055
25	5	26	20	M	0	L	4	3	3	0.00045
26	5	26	20	M	20	M	5	2.4	3.5	0.00036
27	5	26	20	M	40	R	3	2.7	2.5	0.00044

[76].

$$p = 1 - e^{n} \tag{3}$$

In equation (3), p is infection and n is quanta and quanta can be calculated as follows:

$$n = C_{avg} Q_b D \tag{4a}$$

D is the duration of the exposure (h) and Q_b is the volumetric breathing rate of an occupant (m^3/h). C_{avg} is time-average quanta concentration (quanta/m^3) and can be calculated as below:

$$C(t) = \frac{E}{\lambda V}\left(1 - e^{-\lambda t}\right) \tag{5}$$

$$C_{avg} = \int_0^D C(t)dt = \frac{E}{\lambda V}\left[1 - \frac{1}{\lambda D}\left(1 - e^{-\lambda D}\right)\right] \tag{6}$$

In equations (5) and (6), E is quanta emission rate (quanta/h), V is room volume (m^3), λ is first-order loss rate coefficient, and C is the unsteady airborne concentration of infectious quanta (quanta/m^3). λ is the summed effects of ventilation (λ_v, 1/h), gravitational deposition onto surfaces (λ_{dep}, 1/h) and virus decay (k, 1/h):

$$\lambda = \lambda_v + \lambda_{dep} + k \tag{4b}$$

The surface deposition loss rate was 0.3/h [77,78], and virus decay was considered 0.32 1/h [76,79,80]. The quanta emission rate was 0.13 [81] quanta/h (oral breathing) [82], and the breathing rate was 0.54 m^3/h for standing (office, classroom) conditions [83,84].

We applied the Taguchi method to the Wells-Riley equation using the room volume (18, 36, 54 m^3) and inlet velocity values (1, 3, 5 m/s) used in the numerical study. L9(3^2) orthogonal array was used to create an experimental design, as shown in Table 3.

2.6. 2nd case - Constant volume application

Following the completion of the initial numerical study, a smaller office room was examined. In this scenario, a fixed room volume was taken into account. This approach aimed to explore the impact of specific parameters in greater detail, such as inlet velocity, temperature, and manikin position. Additionally, a desktop computer with a monitor and an office desk were included in the model, as depicted in Fig. 2. Similar to the first case, inlet velocity and temperature investigation was conducted within a close range. However, the difference between consecutive values was reduced to observe the parameter's behavior within narrower ranges. Furthermore, the manikin, inlet, and outlet positions were examined at two distinct levels. Investigated parameters for 2nd case are shown in Table 4.

In the second case, the thermal manikin was positioned in front of the table, which was placed adjacent to the center of the wall. Fig. 2 illustrates two different configurations for the manikin, as well as the positions of the inlet and outlet. The room's dimensions were L1 = 3 m, W1 = 2.5 m, and H1 = 2.4 m. The monitor had dimensions of 0.3 m × 0.615 m x 0.015 m, the computer measured 0.15 m × 0.3 m, and the table had dimensions of 0.4 m × 1.2 m x 0.04 m. The table's height from the floor was 0.6 m. The inlet and outlet were located at the center of the wall.

For the inlet velocity, four different values were considered: 1 m/s, 2 m/s, 3 m/s, and 4 m/s, corresponding to air changes per hour (ACH) values of 16, 32, 48, and 64, respectively. Additionally, four different inlet temperatures were investigated: 18 °C, 20 °C, 22 °C, and 24 °C. The range of inlet velocity and temperature was similar to that of the first case, but the difference between consecutive values was decreased to observe the behavior of the parameter within smaller ranges.

An L16 (4^2 2^3) orthogonal array was created for the second case to explore the parameter combinations. The specific configurations of the parameters can be found in Table 5.

2.7. Validation study

For the purpose of validation, the well-known two-dimensional benchmark test case introduced by Nielsen [47] and its corresponding experimental results were employed. As shown in Fig. 3, the validation model consists of a single inlet and outlet, with the

Table 3
L9(3^2) orthogonal array for infection risk calculations.

Case number	Velocity (m/s)	Volume (m^3)	Infection risk (%)
1	1	18	0.186
2	1	36	0.178
3	1	54	0.171
4	3	18	0.064
5	3	36	0.063
6	3	54	0.062
7	5	18	0.039
8	5	36	0.038
9	5	54	0.038

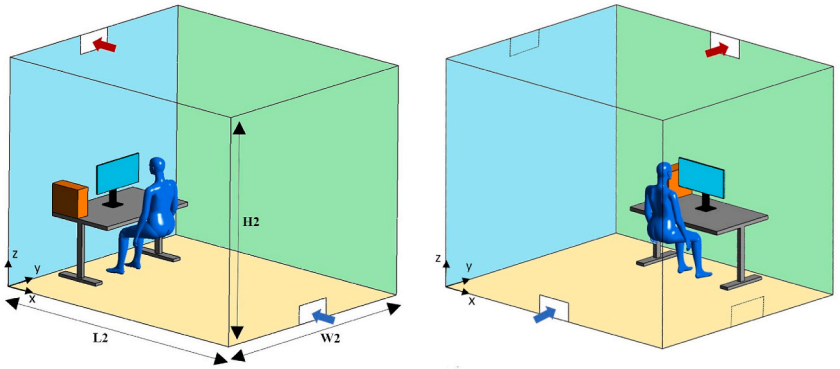

a)1st manikin, inlet and outlet positions. b)2nd manikin, inlet and outlet positions.

Fig. 2. Room model and, inlet and outlet positions for the 2nd case.

Table 4
Parameters and their levels for 2nd case.

Parameters	Levels			
	1	2	3	4
Velocity (m/s)	1	2	3	4
Temperature (°C)	18	20	22	24
Manikin position	1	2		
Inlet location	1	2		
Outlet location	1	2		

Table 5
L16 (4^2 2^3) Orthogonal array for the 2nd case.

Case	Temperature (°C)	Velocity (m/s)	Inlet position	Outlet position	Manikin position	CO_2 (mass fraction)
1	18	1	1	1	1	0.00083
2	18	2	1	1	1	0.00067
3	18	3	2	2	2	0.00060
4	18	4	2	2	2	0.00045
5	20	1	1	2	2	0.00199
6	20	2	1	2	2	0.00078
7	20	3	2	1	1	0.00063
8	20	4	2	1	1	0.00050
9	22	1	2	1	2	0.00135
10	22	2	2	1	2	0.00065
11	22	3	1	2	1	0.00047
12	22	4	1	2	1	0.00037
13	24	1	2	2	1	0.00193
14	24	2	2	2	1	0.00089
15	24	3	1	1	2	0.00048
16	24	4	1	1	2	0.00039

room floor being heated at a low heat flux. In this case, Archimedes' number is Ar = 3.1 × 10-6. The inlet velocity is set at 0.455 m/s in the positive x-direction, and the inlet temperature is 20 °C. The dimensions of the model and the boundary conditions correspond to a Reynolds number of Re = 5000, indicating turbulent airflow within the room. A standard k-ε turbulence model with enhanced wall treatment is implemented to capture the turbulent flow accurately.

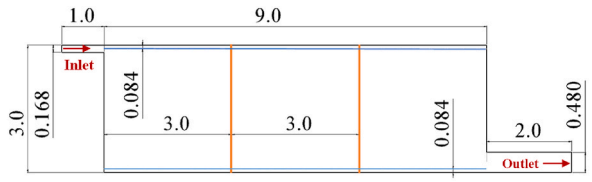

Fig. 3. Dimensions (m) of Annex20 test room.

All walls, except for the floor, are insulated. The thermal interaction between the inlet and the heated bottom surface induces mixed convection within the room. The Boussinesq model is utilized to describe the buoyancy-driven flow occurring in the room. Turbulent flow and mixed convection are representative of the typical flow physics observed in ventilated rooms. Thus, the non-isothermal two-dimensional benchmark test case serves as a suitable means to validate the numerical settings of the primary model.

Non-dimensional velocity profiles at x = 3 m and x = 6 m, and horizontal velocity profiles at y = 0.084 m and y = 2.916 m are shown in Figs. 4 and 5, respectively. The results show that experimental and numerical results are in good agreement. Nielsen performed temperature measurements on the bottom surface, and y = 2.25 m. These experimental data were compared with numerical results in Fig. 6, and these results are also in agreement. Results show that the CFD methodology which was applied to the validation case, could be applied to the main study.

3. Results

A total of 27 cases were generated using an Orthogonal array for the first scenario, aiming to investigate the impact of ventilation parameters on the concentration of the tracer gas within the room. Each simulation provided average concentration values, which are compiled in Table 2.

As anticipated, the inlet velocity is the most influential parameter, accounting for 65.5 % of the variation in CO_2 concentration. Following that, the outlet location (6.3 %), inlet location (6.1 %), and inlet height (5.9 %) were identified as the second, third, and fourth most important parameters, respectively. However, it is worth noting that the delta values of these parameters are very close to each other (1.31, 1.27, 1.24). Hence, considering the numerical error margin, it may not be appropriate to establish a strict hierarchy of importance based solely on these delta values. Instead, it can be assumed that these parameters have a similar effect on CO_2 concentration due to their comparable delta values.

The fifth and sixth important parameters, outlet height (4.5 %) and inlet temperature (4.5 %), exhibit similar delta values with negligible differences, indicating an equivalent impact on CO_2 concentration. Subsequently, the room height (3.1 %), room width (2.4 %), and room length (1.6 %) are identified as the seventh, eighth, and ninth important parameters, respectively.

The impact of ventilation parameters on CO_2 concentration is demonstrated by the variation in the Signal-to-Noise (S/N) ratios for each parameter. Fig. 7 depicts the S/N ratios of each parameter, showcasing the optimal levels for parameter settings. The highest S/N ratio for a given parameter signifies the optimal design level that greatly influences CO_2 concentration.

Based on this approach, the optimal design for achieving the lowest CO_2 concentration entails an inlet velocity of 5 m/s, an inlet temperature of 18 °C, an inlet height of 0.4 m, an “M" inlet position, an outlet distance of 0.2 m, an “M" outlet position, a room length of 5 m, a room height of 3 m, and a room width of 2.5 m. These values represent the numerical setup that is expected to yield the lowest CO_2 concentration. It is important to note that this particular case is not among the 27 cases listed in Table 2. Nevertheless, the numerical solution of this case confirmed the efficacy of this approach, as it resulted in the lowest CO_2 mass fraction value of 0.00030. This outcome further validates the advantage of employing the Taguchi method, which significantly reduces the number of cases required to obtain the optimal setup.

Fig. 8 portrays the CO_2 mass fraction distribution from the CFD solution of the best-case scenario, presented from two different perspectives. The positions of the inlet and outlet correspond to DV, showcasing the advantage of this ventilation type in effectively transporting CO_2 toward the outlet.

The impact of ventilation parameters on pathogen transfer within the room, as depicted in Fig. 7, is not linear. The S/N ratio values reveal that increasing the inlet velocity from 1 m/s to 3 m/s has a more pronounced effect compared to increasing it from 3 m/s to 5 m/s. This finding is significant in terms of energy conservation during ventilation system design. Increasing the inlet velocity was also confirmed by previous studies in the literature to not have had a linear effect on reducing the concentration [38].

Analyzing the S/N ratio values for different temperatures demonstrates that an air temperature of 18 °C is effective in minimizing pathogen mass fraction values. However, it does not imply that higher temperatures always lead to increased mass fraction values. In fact, an inlet air temperature of 26 °C exhibits slightly better performance in reducing mass fraction values compared to 22 °C. This indicates that the airflow pattern within the room is influenced by thermal effects, thereby affecting the distribution of pathogens.

The inlet and outlet locations exhibit similar effects, with direct fresh airflow directed towards the contaminant source proving

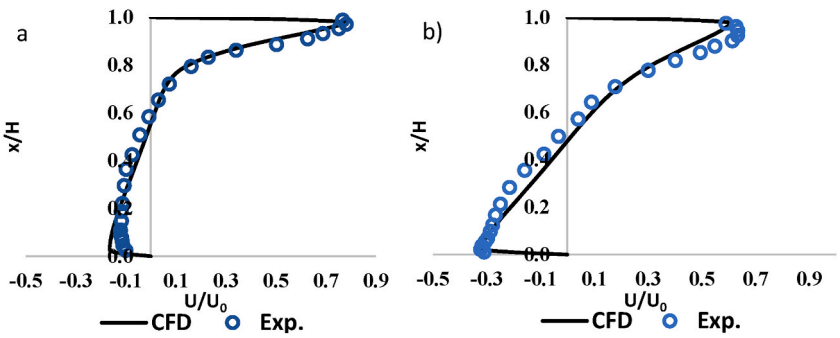

Fig. 4. Non-dimensional velocity distributions at a) x = 3 m, b) x = 6 m

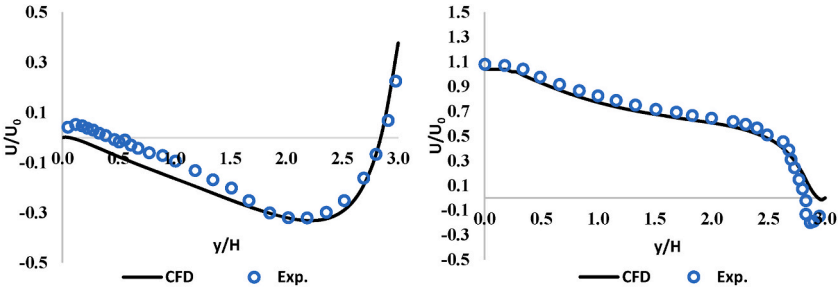

Fig. 5. Non-dimensional velocity distributions at a) y = 0.084 m, b) y = 2.916 m

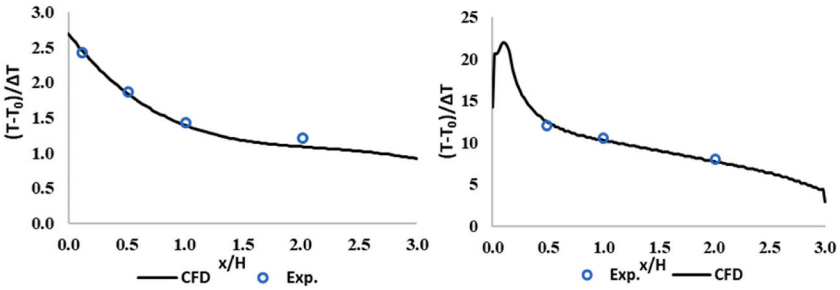

Fig. 6. Non-dimensional temperature distributions at a) y/H = 0.75, b) bottom surface.

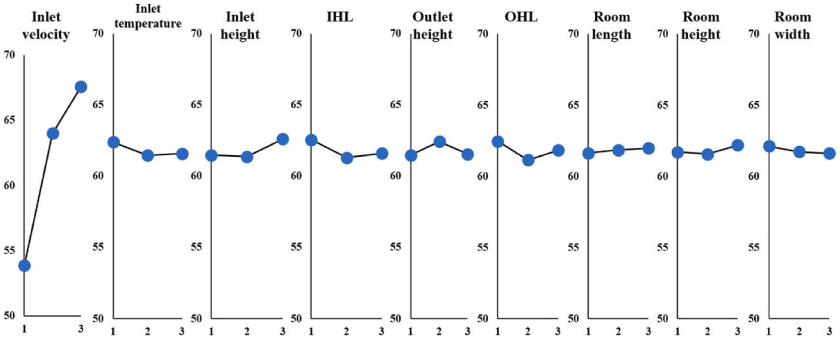

Fig. 7. Effect of each parameter on CO_2 concentration.

more effective than airflow originating from corners. Additionally, extracting indoor air from a location close to the manikin yields better results. Conversely, the vertical height of the inlet and outlet positions demonstrates different behaviors. Increasing or decreasing the vertical height does not have a consistent effect within the range considered in this study, as these differences can influence the airflow pattern within the room.

Interestingly, the dimensions of the room have the least impact on CO_2 mass fraction. This suggests that, in cases with similar airflow patterns, parameters can be selected independently of room dimensions, particularly room size, within certain limits.

The Taguchi method was applied to the Wells-Riley equation using an L9(3^2) orthogonal array. The average Signal-to-Noise (S/N) ratio values obtained from this analysis are presented in Table 7 and visualized in Fig. 9. It is evident, and as expected, that the inlet velocity has a significantly larger effect ratio compared to the room volume.

Statistical analysis results indicate that the inlet velocity contributes to approximately 97.16 % of the infection risk, while the room volume accounts for approximately 2.84 % when both factors are considered together. These findings align closely with the results obtained from the CFD simulations, despite the Wells-Riley method-based calculations not encompassing many of the parameters included in the CFD approach.

Furthermore, the investigation of room volume, considering the dimensions of the room, reveals that the cumulative effect of these dimensions on CO_2 mass fraction amounts to 7.1 % in the CFD results.

In conclusion, despite the methodological differences between the CFD approach and the Wells-Riley method, the consistent effect of room volume and inlet velocity is evident, with the results mutually reinforcing each other.

The average Signal-to-Noise (S/N) ratios were computed for the second case based on each scenario's average CO_2 concentration

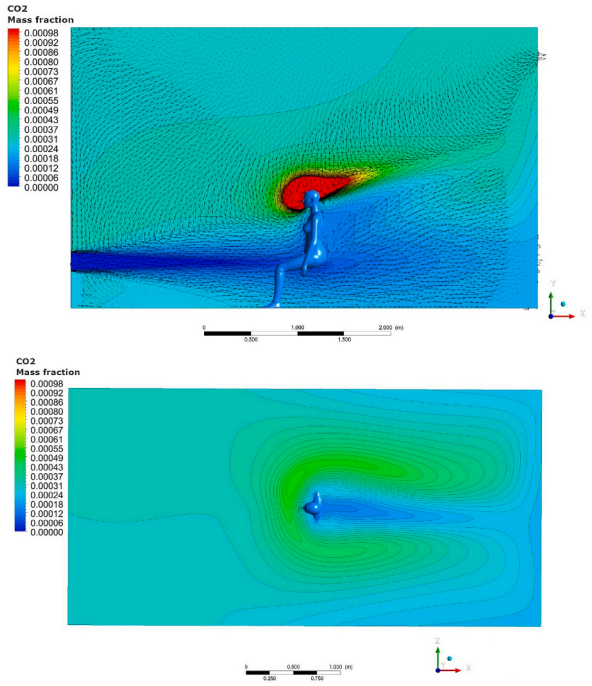

Fig. 8. CO_2 mass fraction distribution of 1st case with velocity vector lines on the a) side view, b) top view.

Table 6
Average S/N ratios and ranking of parameters of CO_2 mass fraction.

Level	Inlet velocity	Inlet temperature	Inlet height	IHL	Outlet height	OHL	Room length	Room height	Room width
1	53.9	62.4	61.5	62.6	61.5	62.5	61.6	61.7	62.1
2	64.0	61.5	61.4	61.3	62.4	61.2	61.9	61.6	61.7
3	67.6	61.6	62.6	61.6	61.6	61.8	62.0	62.2	61.6
Delta	13.7	1.0	1.2	1.3	1.0	1.3	0.3	0.6	0.5
Contribution ratio (%)	65.5	4.5	5.9	6.1	4.5	6.3	1.6	3.1	2.4
Rank	1	6	4	3	5	2	9	7	8

The average Signal-to-Noise (S/N) ratios were computed based on each case's average CO_2 concentration values. These ratios were then utilized to determine the rank of each parameter. Table 6 presents the average S/N ratios, and their corresponding importance ranks. The rank values indicate the order of importance based on the magnitude of the delta values associated with each parameter.

Table 7
Average S/N ratios and ranking of parameters of infection risk.

Level	Inlet velocity	Volume
1	15.0	22.3
2	24.0	22.4
3	28.3	22.6
Delta	13.4	0.4
Contribution ratio (%)	1	2
Rank	97.2	2.8

values. Table 8 presents the average S/N ratios, and their corresponding importance ranks. Once again, the inlet velocity emerges as the most influential parameter, accounting for 63.5 % of the variation in CO_2 concentration, similar to the first case. Despite maintaining a constant room volume and altering the parameters and ranges, the significant impact of air velocity remains consistent with the first case.

In the second case, the second, third, fourth, and fifth important parameters are the inlet temperature (15.6 %), inlet position (9.9 %), outlet position (9.4 %), and manikin position (1.7 %), respectively.

While the first case involved changes in the location of the inlet and outlet on the same walls, the second case features variations in the location of the inlet and outlet across different walls. Despite this difference, the overall effect of changing the inlet and outlet location is comparable in both cases.

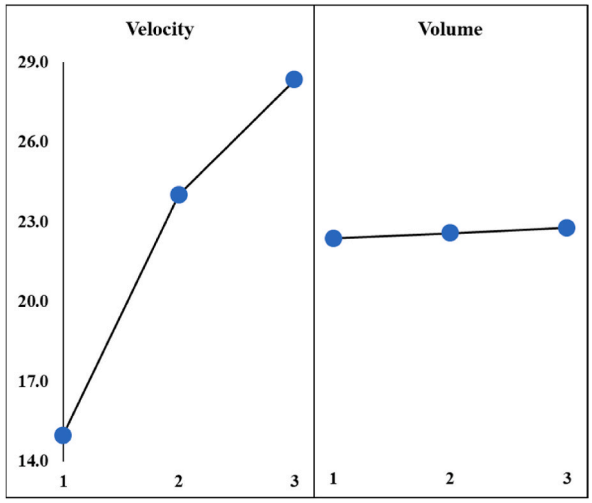

Fig. 9. Effect of room volume and inlet velocity on infection risk.

Table 8
Average S/N ratios and ranking of parameters of CO_2 mass fraction.

Level	Temperature	Velocity	Inlet position	Outlet position	Manikin position
1	64.2	56.8	63.9	63.9	63.2
2	61.5	62.6	62.2	62.3	62.9
3	64.1	65.4			
4	62.5	67.5			
Delta	2.6	10.7	1.7	1.6	0.3
Contribution ratio (%)	15.6	63.5	9.9	9.4	1.7
Rank	2	1	3	4	5

The effect of the inlet temperature is more pronounced in the second case, which has a constant and smaller room volume. Additionally, similar to the first case, the relationship between temperature and CO_2 concentration is non-linear, as evidenced by Fig. 10. Furthermore, there is no distinct temperature pattern observed in relation to concentration. The impact of inlet velocity remains the highest on CO_2 concentration, even in the context of the application with a very small volume, mirroring the findings of the first case.

The graph in Fig. 10 illustrates the variation of each parameter's S/N ratios in relation to CO_2 concentration. For the second case, the optimal design that results in the lowest CO_2 concentration entails an inlet velocity of 4 m/s, an inlet temperature of 18 °C, and the first positions for the inlet, outlet, and manikin, as depicted in Fig. 2. These values represent the optimal numerical setup expected to yield the lowest CO_2 concentration. This specific case is not included in the 16 cases presented in Table 5. This case's numerical solution confirms this approach's effectiveness, with the lowest CO_2 mass fraction value recorded as 0.000156. The CO_2 mass fraction distribution for the best-case scenario in CFD is visualized in Fig. 11 from two different viewpoints.

In contrast to the first case, in the second case, the manikin is positioned facing the air outlet rather than the fresh air inlet, and it is located very close to the outlet. This configuration leads to a lower concentration level compared to the optimal state in the first case. However, when considering the second case independently, the effect of the manikin and table positions on the concentration is relatively low (1.7 %). This effect is also evident in Fig. 11, where the CO_2 concentration behind the manikin appears to be shallow due to the DV airflow pushing the CO_2 concentration away due to inhalation.

4. Discussion

In this study instead of solely focusing on achieving optimal comfort conditions, this study employs the statistical Taguchi method and CFD analysis to analyze the influence of various parameters on indoor airflow dynamics with the aim of minimizing the risk of infection. Understanding the impact ratios of these parameters on pathogen concentration has both practical and theoretical implications. In the field of building and ventilation system design, engineers can use the study's results to prioritize parameters according to their effectiveness. Similarly, researchers can select parameters and objective functions based on the values and impact ratios of the parameters, particularly in multi-objective optimization applications where multiple targets need to be achieved. To encompass a wide range of possibilities, this study considers varying maximum and minimum limits for the parameters, and their variation within this range is assumed to be linear. The advantages and limitations of the statistical method used in this study have been discussed in detail in a previous paper [45].

Average concentration values were employed to assess the risk of infection, and cross-infection is not the focus of this study.

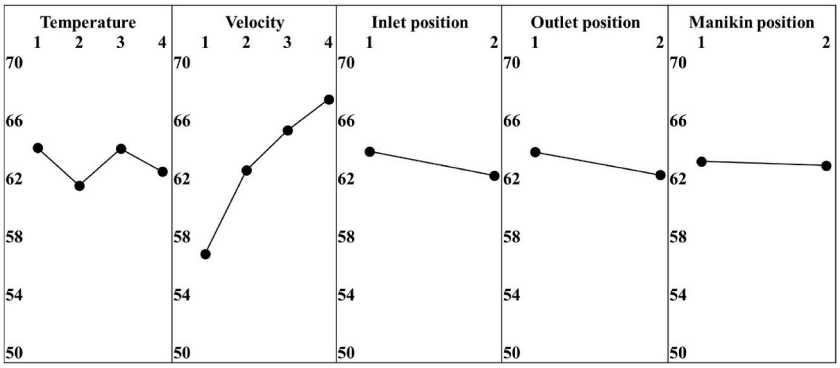

Fig. 10. Effect of each parameter on CO_2 concentration in 2nd case.

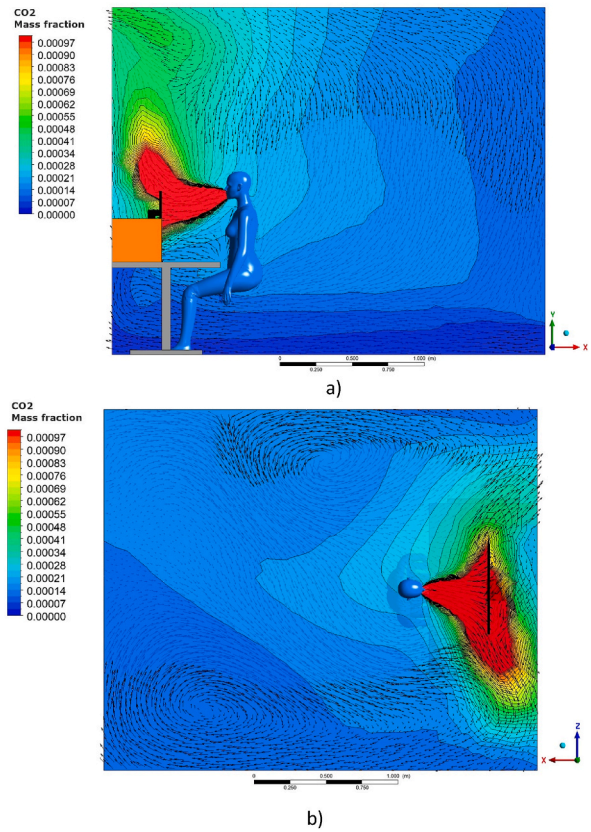

Fig. 11. CO_2 mass fraction distribution of 2nd case with velocity vector lines on the a) side view, b) top view.

However, cross-infection can be investigated in detail in forthcoming research endeavors by incorporating infection risk models. Identifying specific points aimed at reducing infection risk within the objectives will contribute to the literature by facilitating new optimization studies. In future investigations, we intend to employ alternative advanced methodologies, including metaheuristic techniques, to overcome methodological constraints and investigate the effect of other ventilation types.

In our study, we opted for an inlet and outlet configuration aligned with natural airflow patterns due to buoyancy forces, adhering to displacement ventilation principles. This choice was designed to investigate a specific scenario outlined in our manuscript. It's important to acknowledge that our selection does not encompass all possible ventilation solutions for different spaces, particularly those employing alternative air distribution methods. While our computational and methodological constraints confined our investigation to the chosen setup, we remain committed to exploring various ventilation configurations in future studies. These forthcoming investigations aim to provide a more comprehensive understanding of indoor airflow dynamics and their implications for indoor air quality and disease transmission.

The current study did not address the impact of varying quanta emission rates during different vocal activities, as the primary focus remained on room geometry and physical parameters. It should be noted that quanta emission rates can vary among individuals and activities, potentially influencing aerosol dispersion. Nevertheless, the findings related to airflow patterns and proposed solutions retain their relevance for typical breathing scenarios. In future research, exploring different vocal activities is planned to facilitate a more comprehensive understanding of aerosol transmission in various contexts.

While different optimization methods can be employed to analyze parameter variations, they often come with increased computational costs. Therefore, this study suggests using artificial neural networks to establish mathematical relationships between objectives and parameters. These relationships can then be leveraged to apply more cost-effective multi-objective optimization methods.

The findings of this study provide valuable insights for researchers to prioritize the selection of critical parameters and define appropriate objective functions in future studies. Particularly in applying multi-objective optimization methods, these results can guide selecting and effectively optimizing relevant parameters.

Besides the advantages of the statistical method, there are also some limitations to this study. One of the main limitations of this optimization strategy is using an orthogonal array which means the number of parameters and their levels should be consistent with it because experimental designs are constant according to orthogonal arrays in the Taguchi method. Secondly, Parameters are selected as independent from each other to avoid the error of intersecting effects. For example, room volume wasn't used as a different parameter while room dimensions were already used. Therefore, the strategy in this research is eliminating the important parameters according to their effectiveness in concentration and focusing on important parameters by adding new ones in future studies. In addition, there is an error potential in this predictive method and CFD simulations, so we tried to avoid high error values by not using too many parameters in a single study.

5. Conclusions

This study focused on investigating the impact and optimization of ventilation characteristics, including inlet velocity, inlet temperature, positions of the inlet and outlet, and room dimensions (length, width, height), on pathogen transmission in indoor air to ensure healthy indoor environments. The results obtained from this study were further validated using the Wells-Riley method. Subsequently, a smaller room setup was modeled separately, incorporating a seated manikin, table, and computer, using the data collected from the initial study. This novel approach yielded the following significant findings:

- Inlet velocity is the most influential parameter on pathogen transmission among the investigated ventilation parameters. Lower CO_2 mass fraction values were observed at higher velocity values. However, the relationship between velocity and concentration was not linear. Notably, the impact rate of inlet velocity on concentration was consistent across both numerical cases, despite variations in room designs, parameters, and parameter ranges.
- Inlet temperature, inlet-outlet heights and locations, and room height exhibited distinct effects on CO_2 mass fraction at different levels. These findings underscore the significance of conducting optimization studies to establish relationships between these parameters and pathogen transmission. Due to their sensitivity to airflow patterns, predicting these relationships accurately without thorough investigation can be challenging.
- Temperature differences had subtle but independent effects on pathogen transmission in both cases. Particularly in the second case, no specific concentration pattern was associated with temperature. Each level has a different impact, with the second case displaying a higher contribution ratio (15.6 %). The impact of inlet temperature was more pronounced in smaller volumes. Thus, the configuration of ventilation parameters in small indoor environments such as car cabins and elevators holds significance from this perspective.
- Direct airflow directed toward the contaminant source proved to be the most effective solution for reducing pathogen contamination, as observed through the examination of inlet and outlet positions. Optimal positions entailed aligning the inlet and outlet with the manikin. Notably, significantly lower concentration values were obtained when the manikin faced the outlet, even within a small room volume, as evidenced in the second case.
- Room dimensions are the least influential in reducing pathogen concentration Among the investigated parameters, as observed in the first case. The room's length, width, and height had similar effects, suggesting that the impact of room volume on concentration was minimal. This finding aligns with the Wells-Riley equation and implies that ventilation studies addressing airborne transmission within a similar range to this study can be applied to rooms with varying dimensions.

Overall, these findings provide valuable insights into prioritizing focus parameters and defining objective functions in future studies. The optimization of ventilation parameters can be effectively guided by these results, particularly in applying ventilation studies related to airborne transmission in rooms with diverse dimensions.

Credit author statement

Bahadir Erman Yuce: Investigation, Methodology, Writing- Original Draft Preparation, Writing - Review & Editing, Visualization. Amar Aganovic: Writing - Original Draft, Writing - Review & Editing. Peter Vilhelm Nielsen: Writing - Original Draft, Writing - Review & Editing. Pawel Wargocki: Writing - Original Draft, Writing - Review & Editing, Supervision.

Declaration of competing interest

The authors declare the following financial interests/personal relationships which may be considered as potential competing

interests: Bahadir Erman Yuce reports financial support was provided by Scientific and Technological Research Council of Turkey.

Data availability

No data was used for the research described in the article.

References

[1] R. Atiyani, S. Mustafa, S. Alsari, A. Darwish, E.M. Janahi, Clearing the air about airborne transmission of SARS-CoV-2, Eur. Rev. Med. Pharmacol. Sci. 25 (2021) 6745–6766, https://doi.org/10.26355/eurrev_202111_27120.

[2] Z.-W. Ye, S. Yuan, K.-S. Yuen, S.-Y. Fung, C.-P. Chan, D.-Y. Jin, Zoonotic origins of human coronaviruses, Int. J. Biol. Sci. 16 (2020) 1686–1697, https://doi.org/10.7150/ijbs.45472.

[3] D.M. Cutler, L.H. Summers, The COVID-19 pandemic and the $16 trillion virus, JAMA 324 (2020) 1495, https://doi.org/10.1001/jama.2020.19759.

[4] M. Nicola, Z. Alsafi, C. Sohrabi, A. Kerwan, A. Al-Jabir, C. Iosifidis, M. Agha, R. Agha, The socio-economic implications of the coronavirus pandemic (COVID-19): a review, Int. J. Surg. 78 (2020) 185–193, https://doi.org/10.1016/j.ijsu.2020.04.018.

[5] World Health Organization(WHO), Roadmap to Improve and Ensure Good Indoor Ventilation in the Context of COVID-, vol. 19, 2021.

[6] W.F. Wells, ON air-borne infection: study II. Droplets and droplet nuclei, Am. J. Epidemiol. 20 (1934) 611–618, https://doi.org/10.1093/oxfordjournals.aje.a118097.

[7] S. Tang, Y. Mao, R.M. Jones, Q. Tan, J.S. Ji, N. Li, J. Shen, Y. Lv, L. Pan, P. Ding, X. Wang, Y. Wang, C.R. MacIntyre, X. Shi, Aerosol transmission of SARS-CoV-2? Evidence, prevention and control, Environ. Int. 144 (2020), 106039, https://doi.org/10.1016/j.envint.2020.106039.

[8] M. Suleiman, A. Elshaer, M. Billah, M. Bassuony, Propagation of mouth-generated aerosols in a modularly constructed hospital room, Sustainability 13 (2021), 11968, https://doi.org/10.3390/su132111968.

[9] Y. Li, H. Qian, J. Hang, X. Chen, P. Cheng, H. Ling, S. Wang, P. Liang, J. Li, S. Xiao, J. Wei, L. Liu, B.J. Cowling, M. Kang, Probable airborne transmission of SARS-CoV-2 in a poorly ventilated restaurant, Build, Environ. Times 196 (2021), 107788, https://doi.org/10.1016/j.buildenv.2021.107788.

[10] X. Gao, J. Wei, H. Lei, P. Xu, B.J. Cowling, Y. Li, Building ventilation as an effective disease intervention strategy in a dense indoor contact network in an ideal city, PLoS One 11 (2016), e0162481, https://doi.org/10.1371/journal.pone.0162481.

[11] H. Qian, T. Miao, L. Liu, X. Zheng, D. Luo, Y. Li, Indoor transmission of SARS-CoV-2, Indoor Air 31 (2021) 639–645, https://doi.org/10.1111/ina.12766.

[12] M. Mirzaie, E. Lakzian, A. Khan, M.E. Warkiani, O. Mahian, G. Ahmadi, COVID-19 spread in a classroom equipped with partition – a CFD approach, J. Hazard Mater. 420 (2021), 126587, https://doi.org/10.1016/j.jhazmat.2021.126587.

[13] A. Foster, M. Kinzel, Estimating COVID-19 exposure in a classroom setting: a comparison between mathematical and numerical models, Phys. Fluids 33 (2021), 021904, https://doi.org/10.1063/5.0040755.

[14] H. Motamedi, M. Shirzadi, Y. Tominaga, P.A. Mirzaei, CFD modeling of airborne pathogen transmission of COVID-19 in confined spaces under different ventilation strategies, Sustain. Cities Soc. 76 (2022), 103397, https://doi.org/10.1016/j.scs.2021.103397.

[15] A. Magar Mariam, M. Joshi, P.S. Rajagopal, A. Khan, M.M. Rao, B.K. Sapra, CFD simulation of the airborne transmission of COVID-19 vectors emitted during respiratory mechanisms: revisiting the concept of safe distance, ACS Omega 6 (2021) 16876–16889, https://doi.org/10.1021/acsomega.1c01489.

[16] J. Ye, H. Qian, J. Ma, R. Zhou, X. Zheng, Using air curtains to reduce short-range infection risk in consulting ward: a numerical investigation, Build. Simulat. 14 (2021) 325–335, https://doi.org/10.1007/s12273-020-0649-7.

[17] Y. Fan, L. Liu, H. Zhang, Y. Deng, Y. Wang, M. Duan, H. Wang, L. Wang, L. Han, Y. Liu, Exposure of ophthalmologists to patients' exhaled droplets in clinical practice: a numerical simulation of SARS-CoV-2 exposure risk, Front. Public Health 9 (2021), https://doi.org/10.3389/fpubh.2021.725648.

[18] J. Komperda, A. Peyvan, D. Li, B. Kashir, A.L. Yarin, C.M. Megaridis, P. Mirbod, I. Paprotny, L.F. Cooper, S. Rowan, C. Stanford, F. Mashayek, Computer simulation of the SARS-CoV-2 contamination risk in a large dental clinic, Phys. Fluids 33 (2021), 033328, https://doi.org/10.1063/5.0043934.

[19] M. Liu, J. Liu, Q. Cao, X. Li, S. Liu, S. Ji, C.-H. Lin, D. Wei, X. Shen, Z. Long, Q. Chen, Evaluation of different air distribution systems in a commercial airliner cabin in terms of comfort and COVID-19 infection risk, Build. Environ. 208 (2022), 108590, https://doi.org/10.1016/j.buildenv.2021.108590.

[20] Q. Cao, M. Liu, X. Li, C.-H. Lin, D. Wei, S. Ji, T. (Tim), Zhang, Q. Chen, Influencing factors in the simulation of airflow and particle transportation in aircraft cabins by CFD, Build. Environ. 207 (2022), 108413, https://doi.org/10.1016/j.buildenv.2021.108413.

[21] P.S. Desai, N. Sawant, A. Keene, On COVID-19-safety ranking of seats in intercontinental commercial aircrafts: a preliminary multiphysics computational perspective, Build. Simulat. 14 (2021) 1585–1596, https://doi.org/10.1007/s12273-021-0774-y.

[22] Q. Luo, C. Ou, J. Hang, Z. Luo, H. Yang, X. Yang, X. Zhang, Y. Li, X. Fan, Role of pathogen-laden expiratory droplet dispersion and natural ventilation explaining a COVID-19 outbreak in a coach bus, Build. Environ. 220 (2022), 109160, https://doi.org/10.1016/j.buildenv.2022.109160.

[23] C.K. Ho, R. Binns, Modeling and mitigating airborne pathogen risk factors in school buses, Int. Commun. Heat Mass Tran. 129 (2021), 105663, https://doi.org/10.1016/j.icheatmasstransfer.2021.105663.

[24] D. Miller, M. King, J. Nally, J.R. Drodge, G.I. Reeves, A.M. Bate, H. Cooper, U. Dalrymple, I. Hall, M. López-García, S.T. Parker, C.J. Noakes, Modeling the factors that influence exposure to SARS-CoV-2 on a subway train carriage, Indoor Air 32 (2022), https://doi.org/10.1111/ina.12976.

[25] M. Ahmadzadeh, M. Shams, Multi-objective performance assessment of HVAC systems and physical barriers on COVID-19 infection transmission in a high-speed train, J. Build. Eng. 53 (2022), 104544, https://doi.org/10.1016/j.jobe.2022.104544.

[26] H. Li, K. Zhong, Z. (John) Zhai, Investigating the influences of ventilation on the fate of particles generated by patient and medical staff in operating room, Build. Environ. 180 (2020), 107038, https://doi.org/10.1016/j.buildenv.2020.107038.

[27] A.R. Sarhan, P. Naser, J. Naser, COVID-19 aerodynamic evaluation of social distancing in indoor environments, a numerical study, J. Environ. Heal. Sci. Eng. 19 (2021) 1969–1978, https://doi.org/10.1007/s40201-021-00748-0.

[28] G. Pei, M. Taylor, D. Rim, Human exposure to respiratory aerosols in a ventilated room: effects of ventilation condition, emission mode, and social distancing, Sustain. Cities Soc. 73 (2021), 103090, https://doi.org/10.1016/j.scs.2021.103090.

[29] X. Li, Y. Shang, Y. Yan, L. Yang, J. Tu, Modelling of evaporation of cough droplets in inhomogeneous humidity fields using the multi-component Eulerian-Lagrangian approach, Build. Environ. (2018), https://doi.org/10.1016/j.buildenv.2017.11.025.

[30] A. Aganovic, Y. Bi, G. Cao, F. Drangsholt, J. Kurnitski, P. Wargocki, Estimating the impact of indoor relative humidity on SARS-CoV-2 airborne transmission risk using a new modification of the Wells-Riley model, Build. Environ. 205 (2021), https://doi.org/10.1016/j.buildenv.2021.108278.

[31] L. Schumann, J. Lange, Y.E. Cetin, M. Kriegel, Experimental analysis of airborne contaminant distribution in an operating room with different ventilation schemes, Build. Environ. 244 (2023), 110783, https://doi.org/10.1016/j.buildenv.2023.110783.

[32] A. Vlachokostas, C.A. Burns, T.I. Salsbury, R.C. Daniel, D.P. James, J.E. Flaherty, N. Wang, R.M. Underhill, G. Kulkarni, L.F. Pease, Experimental evaluation of respiratory droplet spread to rooms connected by a central ventilation system, Indoor Air 32 (2022), https://doi.org/10.1111/ina.12940.

[33] B. Yang, A.K. Melikov, A. Kabanshi, C. Zhang, F.S. Bauman, G. Cao, H. Awbi, H. Wigö, J. Niu, K.W.D. Cheong, K.W. Tham, M. Sandberg, P.V. Nielsen, R. Kosonen, R. Yao, S. Kato, S.C. Sekhar, S. Schiavon, T. Karimipanah, X. Li, Z. Lin, A review of advanced air distribution methods - theory, practice, limitations and solutions, Energy Build. 202 (2019), 109359, https://doi.org/10.1016/j.enbuild.2019.109359.

[34] H. Skistad, E. Mundt, P.V. Nielsen, K. Hagström, J. Railio, Displacement Ventilation in Non-industrial Premises, second ed., REHVA, 2002.

[35] S. Sadrizadeh, A. Aganovic, A. Bogdan, C. Wang, A. Afshari, A. Hartmann, C. Croitoru, A. Khan, M. Kriegel, M. Lind, Z. Liu, A. Melikov, J. Mo, H. Rotheudt, R. Yao, Y. Zhang, O. Abouali, H. Langvatn, O. Sköldenberg, G. Cao, A systematic review of operating room ventilation, J. Build. Eng. 40 (2021), 102693, https://doi.org/10.1016/j.jobe.2021.102693.

[36] P. V Nielsen, I. Olmedo, M.R. de Adana, P. Grzelecki, R.L. Jensen, Airborne cross-infection risk between two people standing in surroundings with a vertical temperature gradient, HVAC R Res. 18 (2012) 552–561, https://doi.org/10.1080/10789669.2011.598441.
[37] E. Bjørn, P.V. Nielsen, Dispersal of exhaled air and personal exposure in displacement ventilated rooms, Indoor Air 12 (2002) 147–164, https://doi.org/10.1034/j.1600-0668.2002.08126.x.
[38] S. Liu, M. Koupriyanov, D. Paskaruk, G. Fediuk, Q. Chen, Investigation of airborne particle exposure in an office with mixing and displacement ventilation, Sustain. Cities Soc. 79 (2022), 103718, https://doi.org/10.1016/j.scs.2022.103718.
[39] B.P.P. Barbosa, N. de Carvalho Lobo Brum, Ventilation mode performance against airborne respiratory infections in small office spaces: limits and rational improvements for Covid-19, J. Brazilian Soc. Mech. Sci. Eng. 43 (2021) 316, https://doi.org/10.1007/s40430-021-03029-x.
[40] N. Arslanoglu, A. Yigit, Experimental investigation of radiation effect on human thermal comfort by Taguchi method, Appl. Therm. Eng. 92 (2016) 18–23, https://doi.org/10.1016/j.applthermaleng.2015.09.070.
[41] C.-W. Chang, C.-P. Kuo, Evaluation of surface roughness in laser-assisted machining of aluminum oxide ceramics with Taguchi method, Int. J. Mach. Tool Manufact. 47 (2007) 141–147, https://doi.org/10.1016/j.ijmachtools.2006.02.009.
[42] A.M. Pinar, O. Uluer, V. Kırmaci, Optimization of counter flow Ranque–Hilsch vortex tube performance using Taguchi method, Int. J. Refrig. 32 (2009) 1487–1494, https://doi.org/10.1016/j.ijrefrig.2009.02.018.
[43] S. Özel, E. Vural, M. Binici, Optimization of the effect of thermal barrier coating (TBC) on diesel engine performance by Taguchi method, Fuel 263 (2020), 116537, https://doi.org/10.1016/j.fuel.2019.116537.
[44] M. Tutar, H. Aydin, C. Yuce, N. Yavuz, A. Bayram, The optimisation of process parameters for friction stir spot-welded AA3003-H12 aluminium alloy using a Taguchi orthogonal array, Mater. Des. 63 (2014) 789–797, https://doi.org/10.1016/j.matdes.2014.07.003.
[45] B.E. Yuce, P.V. Nielsen, P. Wargocki, The use of Taguchi, ANOVA, and GRA methods to optimize CFD analyses of ventilation performance in buildings, Build. Environ. 225 (2022), 109587, https://doi.org/10.1016/j.buildenv.2022.109587.
[46] Z. (John) Zhai, I.D. Metzger, Taguchi-method-based CFD study and optimisation of personalised ventilation systems, Indoor Built Environ. 21 (2012) 690–702, https://doi.org/10.1177/1420326X11420746.
[47] W. Wang, Z. Tian, Indoor thermal comfort research on the hybrid system of radiant cooling and dedicated outdoor air system, Front. Energy 7 (2013) 155–160, https://doi.org/10.1007/s11708-013-0244-z.
[48] X. Deng, P. Cooper, Z. Ma, G. Kokogiannakis, Numerical analysis of indoor thermal comfort in a cross-ventilated space with top-hung windows, Energy Proc. 121 (2017) 222–229, https://doi.org/10.1016/j.egypro.2017.08.021.
[49] S. Haghshenaskashani, B. Sajadi, M. Cehlin, Multi-objective optimization of impinging jet ventilation systems: Taguchi-based CFD method, Build. Simulat. 11 (2018) 1207–1214, https://doi.org/10.1007/s12273-018-0450-z.
[50] V.R. Lenin, S. Sivalakshmi, M. Raja, Optimization of window type and vent parameters on single-sided natural ventilation buildings, J. Therm. Anal. Calorim. 136 (2019) 367–379, https://doi.org/10.1007/s10973-018-7913-4.
[51] X. Yin, M.W. Muhieldeen, R. Razman, J. Yong Chung Ee, Multi-objective optimization of window configuration and furniture arrangement for the natural ventilation of office buildings using Taguchi-based grey relational analysis, Energy Build. 296 (2023), 113385, https://doi.org/10.1016/j.enbuild.2023.113385.
[52] P.V. Nielsen, Specification of a Two-Dimensional Test Case: (IEA), Inst. Bygningsteknik, Aalborg Univ. R9040, 1990. https://vbn.aau.dk/en/publications/specification-of-a-two-dimensional-test-case-iea.
[53] B.E. Yuce, E. Pulat, Forced, natural and mixed convection benchmark studies for indoor thermal environments, Int. Commun. Heat Mass Tran. 92 (2018) 1–14, https://doi.org/10.1016/j.icheatmasstransfer.2018.02.003.
[54] E. Pulat, H.A. Ersan, Numerical simulation of turbulent airflow in a ventilated room: inlet turbulence parameters and solution multiplicity, Energy Build. 93 (2015) 227–235, https://doi.org/10.1016/j.enbuild.2015.01.067.
[55] T. Liu, Y. Guo, X. Hao, M. Wang, S. He, Z. Lin, R. Zhou, Evaluation of an innovative pediatric isolation (PI) bed using fluid dynamics simulation and aerosol isolation efficacy, Build. Simulat. 14 (2021) 1543–1552, https://doi.org/10.1007/s12273-021-0761-3.
[56] Y. Cengel, M. Boles, Thermodynamics: an Engineering Approach, seventh ed., McGraw-Hill, New York, 2010.
[57] P.V. Nielsen, C. Zhang, L. Liu, Airborne transmission of disease in stratified flow, in: 13TH Nord. Symp. Build. Phys., Aalborg, 2023.
[58] P. V Nielsen, C. Xu, Multiple airflow patterns in human microenvironment and the influence on short-distance airborne cross-infection – a review, Indoor Built Environ. 31 (2022) 1161–1175, https://doi.org/10.1177/1420326X211048539.
[59] J. Ma, X. Qi, H. Chen, X. Li, Z. Zhang, H. Wang, L. Sun, L. Zhang, J. Guo, L. Morawska, S.A. Grinshpun, P. Biswas, R.C. Flagan, M. Yao, Coronavirus disease 2019 patients in earlier stages exhaled millions of severe acute respiratory syndrome coronavirus 2 per hour, Clin. Infect. Dis. 72 (2021) e652–e654, https://doi.org/10.1093/cid/ciaa1283.
[60] R.S. Papineni, F.S. Rosenthal, The size distribution of droplets in the exhaled breath of healthy human subjects, J. Aerosol Med. 10 (1997) 105–116, https://doi.org/10.1089/jam.1997.10.105.
[61] M. Bivolarova, J. Ondráček, A. Melikov, V. Ždímal, A comparison between tracer gas and aerosol particles distribution indoors: the impact of ventilation rate, interaction of airflows, and presence of objects, Indoor Air 27 (2017) 1201–1212, https://doi.org/10.1111/ina.12388.
[62] X. Li, J. Niu, N. Gao, Spatial distribution of human respiratory droplet residuals and exposure risk for the co-occupant under different ventilation methods, HVAC R Res. 17 (2011), https://doi.org/10.1080/10789669.2011.578699.
[63] X. Li, J. Niu, N. Gao, Co-occupant's exposure to exhaled pollutants with two types of personalized ventilation strategies under mixing and displacement ventilation systems, Indoor Air 23 (2013) 162–171, https://doi.org/10.1111/ina.12005.
[64] Y. Yin, W. Xu, J. Gupta, A. Guity, P. Marmion, A. Manning, B. Gulick, X. Zhang, Q. Chen, Experimental study on displacement and mixing ventilation systems for a patient ward, HVAC R Res. 15 (2009) 1175–1191, https://doi.org/10.1080/10789669.2009.10390885.
[65] C. Chen, B. Zhao, Some questions on dispersion of human exhaled droplets in ventilation room: answers from numerical investigation, Indoor Air 20 (2010) 95–111, https://doi.org/10.1111/j.1600-0668.2009.00626.x.
[66] J. Hang, Y. Li, W.H. Ching, J. Wei, R. Jin, L. Liu, X. Xie, Potential airborne transmission between two isolation cubicles through a shared anteroom, Build. Environ. 89 (2015) 264–278, https://doi.org/10.1016/j.buildenv.2015.03.004.
[67] L. Morawska, G.R. Johnson, Z.D. Ristovski, M. Hargreaves, K. Mengersen, S. Corbett, C.Y.H. Chao, Y. Li, D. Katoshevski, Size distribution and sites of origin of droplets expelled from the human respiratory tract during expiratory activities, J. Aerosol Sci. 40 (2009) 256–269, https://doi.org/10.1016/j.jaerosci.2008.11.002.
[68] X. Deng, G. Gong, Effects of indoor air stability on exhaled contaminant flow and thermal plume in the interpersonal breathing microenvironment, Int. J. Therm. Sci. 170 (2021), 107173, https://doi.org/10.1016/j.ijthermalsci.2021.107173.
[69] E. Rivas, J.L. Santiago, F. Martín, A. Martilli, Impact of natural ventilation on exposure to SARS-CoV 2 in indoor/semi-indoor terraces using CO2 concentrations as a proxy, J. Build. Eng. 46 (2022), 103725, https://doi.org/10.1016/j.jobe.2021.103725.
[70] G. Taguchi, Introduction to Quality Engineering, Asian Productivity Organization, Tokyo, 1990.
[71] N. Arslanoglu, A. Yigit, Investigation of efficient parameters on optimum insulation thickness based on theoretical-Taguchi combined method, Environ. Prog. Sustain. Energy 36 (2017) 1824–1831, https://doi.org/10.1002/ep.12628.
[72] P.J. Ross, Taguchi Techniques for Quality Engineering, second, McGraw Hill, New York, 1996.
[73] W.H. Yang, Y.S. Tarng, Design optimization of cutting parameters for turning operations based on the Taguchi method, J. Mater. Process. Technol. 84 (1998) 122–129, https://doi.org/10.1016/S0924-0136(98)00079-X.
[74] A.H. Bademlioglu, A.S. Canbolat, N. Yamankaradeniz, O. Kaynakli, Investigation of parameters affecting Organic Rankine Cycle efficiency by using Taguchi and ANOVA methods, Appl. Therm. Eng. 145 (2018) 221–228, https://doi.org/10.1016/j.applthermaleng.2018.09.032.
[75] G.N. Sze To, C.Y.H.H. Chao, Review and comparison between the Wells-Riley and dose-response approaches to risk assessment of infectious respiratory diseases, Indoor Air 20 (2010) 2–16, https://doi.org/10.1111/j.1600-0668.2009.00621.x.

[76] REHVA, REHVA COVID-19 guidance document, How to operate HVAC and other building service systems to prevent the spread of the coronavirus (SARS-CoV-2) disease (COVID-19) in workplaces, fed, Eur. Heating, Vent. Air Cond. Assoc. (2020).
[77] T.L. Thatcher, A.C.K. Lai, R. Moreno-Jackson, R.G. Sextro, W.W. Nazaroff, Effects of room furnishings and air speed on particle deposition rates indoors, Atmos. Environ. 36 (2002) 1811–1819, https://doi.org/10.1016/S1352-2310(02)00157-7.
[78] E. Diapouli, A. Chaloulakou, P. Koutrakis, Estimating the concentration of indoor particles of outdoor origin: a review, J. Air Waste Manage. Assoc. 63 (2013) 1113–1129, https://doi.org/10.1080/10962247.2013.791649.
[79] A.C. Fears, W.B. Klimstra, P. Duprex, A. Hartman, S.C. Weaver, K.C. Plante, D. Mirchandani, J.A. Plante, P. V Aguilar, D. Fernández, A. Nalca, A. Totura, D. Dyer, B. Kearney, M. Lackemeyer, J.K. Bohannon, R. Johnson, R.F. Garry, D.S. Reed, C.J. Roy, Comparative dynamic aerosol efficiencies of three emergent coronaviruses and the unusual persistence of SARS-CoV-2 in aerosol suspensions, MedRxiv Prepr. Serv. Heal. Sci. (2020), https://doi.org/10.1101/2020.04.13.20063784.
[80] N. van Doremalen, T. Bushmaker, D.H. Morris, M.G. Holbrook, A. Gamble, B.N. Williamson, A. Tamin, J.L. Harcourt, N.J. Thornburg, S.I. Gerber, J.O. Lloyd-Smith, E. de Wit, V.J. Munster, Aerosol and surface stability of SARS-CoV-2 as compared with SARS-CoV-1, N. Engl. J. Med. 382 (2020) 1564–1567, https://doi.org/10.1056/NEJMc2004973.
[81] A. Aganovic, G. Cao, J. Kurnitski, P. Wargocki, New dose-response model and SARS-CoV-2 quanta emission rates for calculating the long-range airborne infection risk, Build. Environ. 228 (2023), 109924, https://doi.org/10.1016/j.buildenv.2022.109924.
[82] G. Buonanno, L. Morawska, L. Stabile, Quantitative assessment of the risk of airborne transmission of SARS-CoV-2 infection: prospective and retrospective applications, Environ. Int. 145 (2020), 106112, https://doi.org/10.1016/j.envint.2020.106112.
[83] B. Binazzi, B. Lanini, R. Bianchi, I. Romagnoli, M. Nerini, F. Gigliotti, R. Duranti, J. Milic-Emili, G. Scano, Breathing pattern and kinematics in normal subjects during speech, singing and loud whispering, Acta Physiol. 186 (2006) 233–246, https://doi.org/10.1111/j.1748-1716.2006.01529.x.
[84] W.C. Adams, Measurement of Breathing Rate and Volume in Routinely Performed Daily Activities, Final Report, 1993.